
HIRL: A General Framework for Hierarchical Image Representation Learning

Minghao Xu^{1,3*} Yuanfan Guo^{2*} Xuanyu Zhu⁴ Jiawen Li⁴ Zhenbang Sun⁴
 Jian Tang^{1,5,6} Yi Xu^{2†} Bingbing Ni^{2†}

*equal contribution †corresponding author

¹Mila - Québec AI Institute

²MoE Key Lab of Artificial Intelligence, AI Institute, Shanghai Jiao Tong University

³University of Montréal ⁴ByteDance ⁵HEC Montréal ⁶CIFAR AI Research Chair

contacts: minghao.xu@umontreal.ca, <gyfastas, xuyi, nibingbing>@sjtu.edu.cn

Abstract

Learning self-supervised image representations has been broadly studied to boost various visual understanding tasks. Existing methods typically learn a single level of image semantics like pairwise semantic similarity or image clustering patterns. However, these methods can hardly capture multiple levels of semantic information that naturally exists in an image dataset, *e.g.*, the semantic hierarchy of “Persian cat → cat → mammal” encoded in an image database for species. It is thus unknown whether an arbitrary image self-supervised learning (SSL) approach can benefit from learning such hierarchical semantics. To answer this question, we propose a general framework for **Hierarchical Image Representation Learning (HIRL)**. This framework aims to learn multiple semantic representations for each image, and these representations are structured to encode image semantics from fine-grained to coarse-grained. Based on a probabilistic factorization, HIRL learns the most fine-grained semantics by an off-the-shelf image SSL approach and learns multiple coarse-grained semantics by a novel **semantic path discrimination** scheme. We adopt six representative image SSL methods as baselines and study how they perform under HIRL. By rigorous fair comparison, performance gain is observed on all the six methods for diverse downstream tasks, which, for the first time, verifies the general effectiveness of learning hierarchical image semantics. All source code and model weights are available at <https://github.com/hirl-team/HIRL>.

1 Introduction

Self-supervised image representation learning has been enthusiastically studied in recent years. It focuses on acquiring informative and interpretable feature representations for unlabeled images, where the learning signal totally comes from the data itself. To attain this goal, a variety of self-supervised learning (SSL) techniques have been developed to capture different levels of semantics underlying the raw images, *e.g.*, capturing the semantic similarity between image pairs [25, 11, 14, 16] and capturing the semantics of image clusters [5, 7, 32, 8]. The image representations learned by these methods have been proven to be effective on various downstream tasks, and the performance gap between SSL and fully-supervised learning is continually narrowing.

However, for modeling a large-scale image dataset, it is always not enough to capture a single level of semantic information, because of the fact that such a dataset commonly contains multiple semantic hierarchies. For example, in a dataset of diverse species, an image of *Persian cat* also owns a more coarse-grained semantics of *cat* and an even more coarse-grained semantics of *mammal*. Encoding such hierarchical semantic information (*e.g.*, Persian cat → cat → mammal) in image representations can broadly benefit different downstream tasks, *e.g.*, image classification with different

label granularity. There are some recent works [6, 32, 23] aiming to learn such hierarchical semantic representations, and some performance gain has been verified by incorporating such a scheme. However, there still lacks a systematic study on **whether any off-the-shelf image SSL method can benefit from learning multiple levels of semantic information**.

To answer this question, in this work, we propose a general framework for **Hierarchical Image Representation Learning (HIRL)**. This framework seeks to learn multiple representations for each image, and these representations encode the image’s different levels of semantics from fine-grained to coarse-grained. To set up a starting point of this semantic hierarchy, we employ an arbitrary off-the-shelf image SSL method to learn the representation of the most fine-grained semantics. On such basis, we propose a novel **semantic path discrimination (SPD)** approach to learn the representations of more coarse-grained semantics. This approach first identifies some representative embeddings (*i.e.*, prototypes) of underlying semantic clusters on different semantic levels. For each image, it then retrieves a positive path composed of the prototypes with the same hierarchical semantics as the image and retrieves multiple negative paths composed of the prototypes that encode different semantics with the image. The objective of SPD is to maximize the similarity between the image’s hierarchical representations and the positive path while minimize the similarity between the hierarchical representations and the negative paths. In this way, the HIRL framework can incorporate the objective of hierarchical semantic representation learning into various off-the-shelf image SSL methods, which strengthens their capability of modeling image semantics.

For fair comparison, we first re-implement three representative CNN based SSL algorithms and three representative Vision Transformer based SSL algorithms under a common codebase. We then adapt these six image SSL methods to the HIRL framework and compare their performance before and after enabling hierarchical semantic modeling. The experimental results on standard downstream evaluation tasks, *e.g.*, KNN evaluation, linear classification and fine-tuning on ImageNet [18], verify that the effectiveness of six image SSL baselines are all improved by learning hierarchical semantic information. Based on such comprehensive comparisons, we suggest HIRL as a general framework that can boost a wide range of image SSL approaches by learning hierarchical image semantics.

2 Related Work

CNN based self-supervised image representation learning. Self-supervised learning (SSL) methods have been broadly studied to acquire effective image representations. Most of the prevailing approaches in this area are designed upon CNN architectures (*e.g.*, ResNet [27]). In this line of research, most early works [49, 31, 21, 37] focus on designing useful pretext tasks. Breakthroughs have been witnessed in this area since the introduction of *contrastive learning* [41, 43, 25, 11, 14]. The key idea of contrastive learning is to embed similar instances nearby in the latent space while embed dissimilar ones distantly. Such an objective is commonly pursued by minimizing the InfoNCE loss [41, 29]. Recent works seek to improve the standard contrastive learning scheme by relieving the reliance on negative sampling [22, 15, 48], capturing the semantic information of image clusters [7, 32, 23], utilizing stronger augmentation functions [7, 42] or selecting better positive and negative pairs [17, 30, 12]. These efforts enable the CNN model learned with self-supervision to have competitive performance with its fully-supervised counterpart.

Vision Transformer based self-supervised image representation learning. The development of different Vision Transformers [20, 40, 35] revolutionize the basic architecture of image encoders. These architectures require specific schemes for self-supervised learning. Inspired by the masked language modeling (MLM) approach [19] for pre-training text Transformers, masked image modeling (MIM) based methods [10, 3, 24, 45, 51] are proposed to learn self-supervised image representations with Vision Transformers. Besides MIM, self-distillation [8, 51, 2, 13] and contrastive learning [16] based objectives are also explored for the SSL of Vision Transformers. The performance of these approaches is catching up with fully-supervised learning.

Hierarchical image representation learning. Our work is closely related to the previous works [44, 46, 5, 6, 1, 7, 32, 23] for simultaneous image clustering and representation learning. Most of these works [44, 46, 5, 1, 7] learn a single level of semantics for an image dataset, which cannot capture the hierarchical semantic information that naturally exists underlying the images. Some recent works [6, 32, 23] make an attempt on learning such hierarchical semantics, and they have achieved performance gain by injecting into specific SSL baselines. However, there still lacks a systematic study on whether hierarchical image representation learning can enhance various existing image SSL methods under different model architectures.

To answer this question, this work proposes a general framework for hierarchical image representation learning, named as HIRL. Inspired by a probabilistic factorization, this framework naturally embraces the objective of an arbitrary off-the-shelf image SSL method and the objective for learning hierarchical semantic information. Under the HIRL framework, performance gain is observed on six representative image SSL methods (three CNN based and three Vision Transformer based), which, for the first time, verifies the general effectiveness of learning multiple levels of image semantics.

3 Problem Definition and Preliminary

3.1 Problem Definition

Upon a set $X = \{x_1, x_2, \dots, x_N\}$ of N raw images without label information, we seek to learn a *hierarchical representation* z_n for each image $x_n \in X$. Specifically, we consider $L + 1$ latent spaces $\{V_l\}_{l=0}^L$ that represent different levels of semantic information, and these latent semantics are desired to be organized in a *fine-to-coarse* way, *i.e.*, representing the most fine-grained semantics in the space V_0 and representing gradually more coarse-grained semantics in the remaining L spaces. In this way, we represent each image with a chain $z_n = \{z_n^l\}_{l=0}^L$ of low-dimensional vectors, where $z_n^l \in \mathbb{R}^d$ denotes the representation of image x_n in the semantic space V_l . Following the philosophy of self-supervised learning, the hierarchical image representations $Z = \{z_1, z_2, \dots, z_N\}$ are learned under the supervision of the data itself.

3.2 Preliminary

Hierarchical prototypes. The learning of hierarchical image representations is guided by hierarchical prototypes [23], *i.e.*, the representative embeddings of semantic clusters on different semantic levels, denoted as $\mathcal{C} = \{\{c_i^l\}_{i=1}^{M_l}\}_{l=1}^L$ (L : number of semantic levels; M_l : number of prototypes at the l -th semantic level). These prototypes are obtained by the hierarchical K-means algorithm [23], as summarized in Alg. 1. To start this procedure, we extract the vanilla image representations without hierarchical semantics by an image encoder, *e.g.*, the average pooled embedding from ResNet [27] or the [CLS] token embedding from ViT [20], denoted as $\tilde{Z} = \{\tilde{z}_1, \tilde{z}_2, \dots, \tilde{z}_N\}$. A standard K-means clustering is applied upon these image representations to derive the prototypes at the first semantic level. After that, the K-means clustering is iteratively applied to the prototypes at the current semantic level to get the prototypes at a more coarse-grained semantic level. The cluster assignment relations between two consecutive levels of prototypes are stored as an edge set \mathcal{E} , which structures hierarchical prototypes as a set of trees (Fig. 1(a) shows such a tree). The hierarchical prototypes derived in this way form a fine-to-coarse semantic hierarchy, which is suitable to guide the learning of hierarchical image representations.

Algorithm 1 Hierarchical K-means.

Input: Vanilla image representations \tilde{Z} .
Output: Hierarchical prototypes $\mathcal{C} = \{\{c_i^l\}_{i=1}^{M_l}\}_{l=1}^L$, the set \mathcal{E} of edges between different prototypes.
 $\{c_i^1\}_{i=1}^{M_1} \leftarrow \text{K-means}(\tilde{Z})$.
for $l = 2$ **to** L **do**
 $\{c_i^l\}_{i=1}^{M_l} \leftarrow \text{K-means}(\{c_i^{l-1}\}_{i=1}^{M_{l-1}})$.
 for $i = 1$ **to** M_{l-1} **do**
 $\mathcal{E} \leftarrow \mathcal{E} \cup \{(c_i^{l-1}, \text{AssignedPrototype}(c_i^l))\}$.
 end for
end for

4 Hierarchical Image Representation Learning

In this section, we introduce the framework of hierarchical image representation learning (HIRL). This framework models hierarchical image representations in a factorized way, *i.e.*, the modeling at the most fine-grained semantic level and the modeling at more coarse-grained semantic levels (Sec. 4.1). The first modeling problem can be solved by any off-the-shelf image SSL method, and the second modeling problem is solved by a novel *semantic path discrimination* approach (Sec. 4.2). By combining these two kinds of objectives, HIRL can enhance existing image SSL methods through better capturing hierarchical semantic information (Sec. 4.3).

4.1 Probabilistic Formalization

Given an image x , we aim to model its hierarchical representations $z = \{z^l\}_{l=0}^L$ that encode its semantic information in a fine-to-coarse way. Directly modeling the joint distribution $p(z^0, \dots, z^L | x)$ of all semantic representations is hard, since there lacks a concept of the most fine-grained semantics

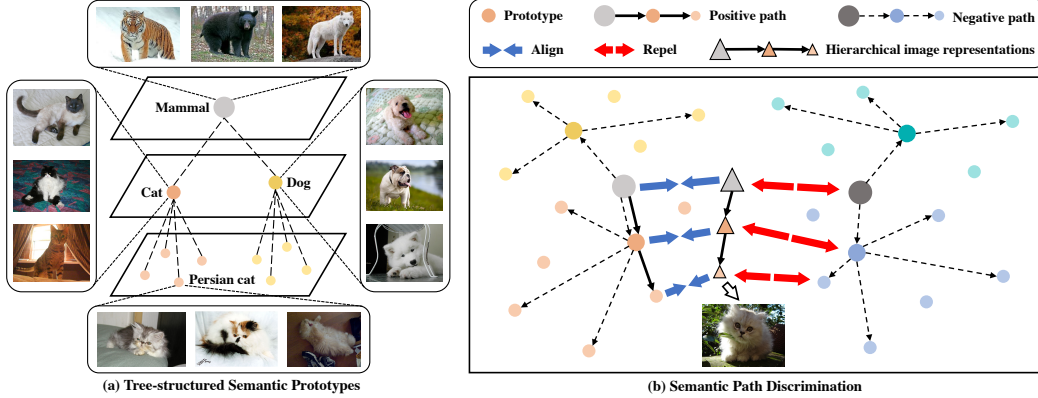


Figure 1: **Illustration of HIRL framework.** (a) Tree-structured semantic prototypes are constructed to guide the learning of hierarchical semantics of images. (b) Semantic path discrimination learns hierarchical image representations by aligning the representations with the corresponding positive semantic path while repelling the representations from negative semantic paths.

that we should start from. Therefore, the HIRL framework solves this problem in a factorized way, *i.e.*, first modeling $p(z^0|x)$ to set up the most fine-grained semantic representation and then modeling the joint distribution $p(z^1, \dots, z^L|z^0)$ for more coarse-grained semantics:

$$p(z^0, \dots, z^L|x) = p(z^0|x)p(z^1, \dots, z^L|z^0). \quad (1)$$

The first term $p(z^0|x)$ can be suitably modeled by off-the-shelf image SSL methods, since they are designed to capture a single level of semantic information, *e.g.*, by modeling the dependency among image patches [24, 51], capturing the semantic similarity between image pairs [14, 16] or modeling image clustering patterns [7, 8]. However, the modeling of the second term $p(z^1, \dots, z^L|z^0)$ for hierarchical semantic representations is non-trivial, which requires to capture the dependency of coarse-grained semantics on fine-grained semantics and also the interdependency among different levels of coarse-grained semantics. We introduce our solution in the next part.

4.2 Semantic Path Discrimination

In HIRL, we regard the image representation learned by an off-the-shelf SSL method as the most fine-grained semantic representation z^0 that lies in the space V_0 . On such basis, we further learn hierarchical semantic representations $\{z^l\}_{l=1}^L$ to improve model’s representation learning ability.

Hierarchical representation derivation. Upon the representation z^0 , we utilize an MLP projection head $h_l : V_0 \rightarrow V_l$ to map it onto the semantic space V_l representing more coarse-grained semantics, *i.e.*, $z^l = h_l(z^0)$ ($1 \leq l \leq L$). Learning these hierarchical representations requires some guidance on what specific semantic information should be encoded in each representation. We resort to *hierarchical prototypes* (Sec. 3.2) for such guidance. These prototypes serve as the anchor points that locate potential semantic clusters on different semantic spaces. In the derivation of hierarchical prototypes (Alg. 1), we set $\tilde{Z} = \{z_1^0, z_2^0, \dots, z_N^0\}$ to guarantee that the modeling of coarse-grained semantics is based on the most fine-grained one, *i.e.*, modeling $p(z^1, \dots, z^L|z^0)$ faithfully.

The other important part of modeling $p(z^1, \dots, z^L|z^0)$ is to model the *joint likelihood* of hierarchical semantic representations $\{z^l\}_{l=1}^L$ for a specific sample. To perform such joint modeling, we employ the consecutive prototypes (*i.e.*, paths) in hierarchical prototypes as references and seek to align the representations $\{z^l\}_{l=1}^L$ as a whole with the most likely path for each sample.

Semantic path retrieval. In hierarchical prototypes, we define a *semantic path* $\mathbb{P} = \{c^l\}_{l=1}^L$ as a path traversing from a bottom layer prototype c^1 to its corresponding top layer prototype c^L based on the tree structure. Such a path represents some hierarchical semantics underlying the data, like Persian cat \rightarrow cat \rightarrow mammal, which is desired to be encoded in hierarchical representations $\{z^l\}_{l=1}^L$.

Given an image x , we define two kinds of paths in hierarchical prototypes, *i.e.*, the *positive path* and the *negative path*, to learn its representations. The prototypes on the positive path encode the same semantics as x on each semantic level, while the prototypes on the negative path could encode

different semantics with x on some semantic level. We extract the positive path $\mathbb{P}_+ = \{c_+^l\}_{l=1}^L$ by first retrieving the bottom layer prototype c_+^1 that the image is assigned to during K-means clustering (the first step in Alg. 1) and then traversing from bottom to top. A negative path $\mathbb{P}_- = \{c_-^l\}_{l=1}^L$ starts from any bottom layer prototype c_-^1 other than c_+^1 and traverses from bottom to top. Note that, there exists a single positive path and $M_1 - 1$ possible negative paths for each image.

Semantic path discrimination. Based on these definitions, we formalize the semantic path discrimination problem as maximizing the similarity between hierarchical representations $\{z^l\}_{l=1}^L$ and the positive path, while minimizing the similarity between these representations and the negative path. To measure the similarity between hierarchical representations $\{z^l\}_{l=1}^L$ and a semantic path $\mathbb{P} = \{c^l\}_{l=1}^L$, we compute the similarity between each corresponding pair (z^l, c^l) of representation and prototype and multiplying across all pairwise similarities:

$$s(\{z^l\}_{l=1}^L, \mathbb{P}) = \prod_{l=1}^L \frac{1 + \cos(z^l, c^l)}{2}, \quad (2)$$

where we map each cosine similarity $\cos(z^l, c^l)$ to $[0, 1]$ for similarity multiplication. We randomly sample N_{neg} negative paths from all possible negative paths, and the objective function of semantic path discrimination is formalized as a balanced binary classification loss:

$$\mathcal{L}_{\text{SPD}}(\theta) = -\mathbb{E}_{x \sim p_d} \left[\log \left(s(\{z^l\}_{l=1}^L, \mathbb{P}_+) \right) + \frac{1}{N_{\text{neg}}} \sum_{k=1}^{N_{\text{neg}}} \log \left(1 - s(\{z^l\}_{l=1}^L, \mathbb{P}_-^k) \right) \right], \quad (3)$$

where θ denotes all model parameters including the parameters of image encoder and projection heads, and p_d is the data distribution that all images are drawn from. We provide a graphical illustration of semantic path discrimination in Fig. 1.

Overall objective. Under the HIRL framework, the joint distribution $p(z^0, \dots, z^L | x)$ of all semantic representations is modeled in a factorized way. The objective function \mathcal{L}_{img} of an off-the-shelf image SSL method models the distribution $p(z^0 | x)$ for the most fine-grained semantics, and the objective function \mathcal{L}_{SPD} of semantic path discrimination models the distribution $p(z^1, \dots, z^L | z^0)$ for more coarse-grained semantics. The overall objective combines these two objectives to learn the hierarchical image representations on all considered semantic levels:

$$\min_{\theta} \mathcal{L}_{\text{img}}(\theta) + \mathcal{L}_{\text{SPD}}(\theta). \quad (4)$$

4.3 Pre-training and Downstream Application

Pre-training. The pre-training under HIRL is performed by two stages, as summarized in Alg. 2. In the first stage, the image encoder is trained with only \mathcal{L}_{img} to learn the most fine-grained semantic representation z^0 , which sets up the basic concepts about image semantics. At the start of each epoch in the second stage, a hierarchical K-means step is performed upon the image representations $\tilde{Z} = \{z_1^0, z_2^0, \dots, z_N^0\}$ extracted by the current encoder to update hierarchical prototypes, which balances between training efficiency and the accuracy of hierarchical prototypes as representative cluster embeddings. Its time complexity is analyzed in Sec. 6.2. In the second stage, \mathcal{L}_{img} and \mathcal{L}_{SPD} are jointly applied to train the encoder and projection heads, which facilitates the model to capture the hierarchical semantics of images. By comparison, existing image SSL methods mainly focus on capturing a single level of semantic information and are thus less effective.

Downstream application. After pre-training under the HIRL framework, we can obtain a strong image encoder whose output representation z^0 can (1) encode fine-grained semantics by the modeling of $p(z^0 | x)$ and also (2) implicitly encode different levels of coarse-grained semantic information by the modeling of $p(z^1, \dots, z^L | z^0)$. Because of such merits, in downstream applications, we can discard the projection heads used in pre-training and only use the image encoder for feature extraction, which guarantees the transportability of the pre-trained model on various downstream tasks.

Algorithm 2 The learning procedure of HIRL.

Input: Unlabeled images X , first-stage training epochs T_1 , second-stage training epochs T_2 .

Output: Pre-trained model F_{θ} .

Train the model with only \mathcal{L}_{img} for T_1 epochs.

for $t = 1$ **to** T_2 **do**

$\tilde{Z} \leftarrow F_{\theta}(X)$.

$\mathcal{C} \leftarrow \text{Hierarchical_K-means}(\tilde{Z})$.

Train the model with \mathcal{L}_{img} and \mathcal{L}_{SPD} for one epoch.

end for

5 Experiments

5.1 Implementation Details

5.1.1 Image SSL Baselines

We adopt three representative CNN based image SSL methods (*i.e.*, MoCo v2 [14], SimSiam [15] and SwAV [7]) and three representative Vision Transformer based image SSL methods (*i.e.*, MoCo v3 [16], DINO [8] and iBOT [51]) as baselines. To facilitate fair comparison and reproducibility, under PyTorch [38] (BSD License), we re-implement these baselines and associated downstream tasks in a unified codebase (<https://github.com/hirl-team/HIRL>). We briefly introduce these baselines from the perspective of learning image semantics as below:

- **MoCo v2 [14]** (*CNN based*) is a typical approach to acquire the semantic similarity of image pairs. It employs a standard contrastive learning scheme to maximize the similarity of correlated image pairs while minimize the similarity of uncorrelated image pairs.
- **SimSiam [15]** (*CNN based*) is another popular method that learns pairwise semantic similarity. Instead of contrasting between positive and negative pairs as in MoCo v2, SimSiam directly maximizes the similarity between correlated (*i.e.*, positive) image pairs, using no negative pairs. It introduces a stop-gradient scheme to avoid collapsed representations.
- **SwAV [7]** (*CNN based*) is a superior image SSL approach for CNNs, which learns the semantic information encoded in a single hierarchy of image clusters. It designs a swapped prediction problem to predict the cluster assignment of a view of an image from its another view. It proposes a multi-crop augmentation scheme to further enhance model’s performance.
- **MoCo v3 [16]** (*Vision Transformer based*) can be regarded as a variant of MoCo v2 under Vision Transformer architectures, and it also learns pairwise semantic similarity. To stabilize the training process of SSL, it proposes a bunch of implementation suggestions that work well in practice.
- **DINO [8]** (*Vision Transformer based*) learns image representations by self-distillation, *i.e.*, aligning the categorical distribution output by a student network with that of a teacher network. In this way, DINO captures the semantics underlying a single hierarchy of image clusters.
- **iBOT [51]** (*Vision Transformer based*) employs a masked image modeling objective and a self-distillation objective. The masked image modeling objective seeks to align the categorical distribution of the same patch that is masked or unmasked in an image, and the self-distillation objective follows the one in DINO. By simultaneously optimizing these two objectives, iBOT can capture the semantic information encoded in a single hierarchy of image/patch clusters.

5.1.2 Adaptation to the HIRL Framework

To study the effect of learning multiple levels of extra semantic information, we adapt each baseline method into the proposed HIRL framework and compare the performance before and after such adaptation. During adaptation, we follow the principle that all the model architectures, training procedures and hyperparameter settings of the baseline method are unchanged, such that fair comparison is ensured. The interaction between the baseline method and the HIRL framework mainly lies in two aspects, *feature extraction* and *loss computation*, which we briefly introduce here and leave more details in Sec. A.1.

Feature extraction. Under the HIRL framework, we utilize the encoder of baseline to extract image representations \tilde{Z} for the per-epoch hierarchical K-means step (Alg. 2), and these representations also serve as the inputs of the projection heads h_l ($1 \leq l \leq L$) for hierarchical semantic representations (Sec. 4.2). For MoCo v2, SimSiam and SwAV, each $\tilde{z} \in \tilde{Z}$ is the projected representation of the average pooled embedding from ResNet [27]. For MoCo v3, DINO and iBOT, each $\tilde{z} \in \tilde{Z}$ is the projected representation of the [CLS] token embedding from ViT [20]. We employ the momentum encoder of MoCo v2 and the teacher network of DINO and iBOT for feature extraction, since they are used for downstream evaluation in official implementations.

Loss computation. In the second training stage of HIRL (Alg. 2), we optimize the image encoder and the projection heads by a joint loss (Eq. (4)) that combines the loss \mathcal{L}_{img} of baseline and the loss \mathcal{L}_{SPD} for learning hierarchical semantic representations.

Table 2: Training environments and performance comparison on KNN evaluation (Top1-Acc), linear classification (Top1-Acc), fine-tuning (Top1-Acc) and semi-supervised learning with 1% or 10% data (Top1-Acc). We use Tesla-V100-32GB GPUs for all experiments.

Method	Arch.	# Epochs	Batch size	# GPUs	Train time	KNN	Linear	Fine-tune	Semi-1%	Semi-10%
CNN based image SSL methods										
MoCo v2	ResNet-50	200	256	8	45h 23min	55.74	67.60	73.14	35.96	60.6
HIRL-MoCo v2	ResNet-50	200	256	8	58h 50min	57.56 (↑1.82)	68.40 (↑0.8)	73.86 (↑0.72)	37.31 (↑1.35)	61.71 (↑1.11)
SimSiam	ResNet-50	200	512	16	40h 32min	60.17	69.74	72.25	31.04	61.55
HIRL-SimSiam	ResNet-50	200	512	16	70h 30min	62.68 (↑2.51)	69.81 (↑0.07)	72.88 (↑0.63)	33.34 (↑2.30)	62.94 (↑1.39)
SwAV	ResNet-50	200	4096	32	20h 15min	63.45	72.68	76.82	51.23	68.72
HIRL-SwAV	ResNet-50	200	4096	32	27h 45min	63.99 (↑0.54)	73.43 (↑0.75)	77.18 (↑0.36)	52.12 (↑0.89)	69.32 (↑0.60)
Vision Transformer based image SSL methods										
MoCo v3	ViT-B/16	400	4096	128	26h 18min	71.29	76.44	81.94	58.01	75.20
HIRL-MoCo v3	ViT-B/16	400	4096	128	45h 20min	71.68 (↑0.39)	75.12 (↓1.32)	82.19 (↑0.25)	60.92 (↑2.91)	74.91 (↓0.29)
DINO	ViT-B/16	400	1024	32	86h 40min	76.01	78.07	82.09	62.35	76.57
HIRL-DINO	ViT-B/16	400	1024	32	107h 40min	76.84 (↑0.83)	78.32 (↑0.25)	83.24 (↑1.15)	64.73 (↑2.38)	76.85 (↑0.28)
iBOT	ViT-B/16	400	1024	32	87h 20min	76.64	79.00	82.47	64.60	77.19
HIRL-iBOT	ViT-B/16	400	1024	32	108h 20min	77.49 (↑0.85)	79.36 (↑0.36)	83.37 (↑0.90)	66.15 (↑1.55)	77.32 (↑0.13)

5.1.3 Model Details

To fairly compare different CNN or Vision Transformer based SSL methods, we set ResNet-50 [27] as the encoder for MoCo v2, SimSiam and SwAV and set ViT-B/16 [20] as the encoder for MoCo v3, DINO and iBOT. The projection heads h_l ($1 \leq l \leq L$) are implemented as 2-layer MLPs with batch normalization and ReLU activation in between (for MoCo v3, 5-layer MLPs are used for better convergence). We use the same representation dimension d for all semantic spaces $\{V_l\}_{l=0}^L$ (Tab. 6 lists the dimension of each method). For each combination of a baseline method and HIRL, we set its number of semantic levels as $L = 3$, and we search for its prototype numbers among $(M_1, M_2, M_3) \in \{(30000, 10000, 1000), (30000, 10000, 5000)\}$ and its negative path sampling size among $N_{\text{neg}} \in \{100, 1000\}$. For this search, we hold out 8,000 ImageNet [18] training samples for validation and select the configuration with the lowest joint loss (Eq. (4)) on this validation split. The search results are shown in Tab. 1. We do ablation studies for L , $\{M_l\}_{l=1}^L$ and N_{neg} in Sec. 6.1.

5.1.4 Training Details

For both a baseline and its variant under the HIRL framework, we totally follow its official implementation to set the optimizer, learning rate and learning rate scheduler, and the detailed setups for each baseline are listed in Sec. A.2. We train three CNN based approaches for 200 epochs and train three Vision Transformer based approaches for 400 epochs. The official SwAV suggests 800 epochs training for better performance, which we provide in Sec. B. The number of first-stage training epochs (*i.e.*, T_1 in Alg. 2) is set as 20 for MoCo v2, SimSiam, SwAV and MoCo v3 and is set as 40 for DINO and iBOT, and the second-stage training takes the rest epochs. We list the training batch size, GPU number and training time of each method in Tab. 2.

5.2 Experimental Results¹

5.2.1 KNN Evaluation, Linear Classification and Fine-tuning

Evaluation Setups. All the three tasks are evaluated on the ImageNet dataset [18]. *KNN evaluation* predicts each sample’s label based on the labels of its nearest neighbors. We follow NPID [43] to report the highest KNN classification accuracy among $K \in \{10, 20, 100, 200\}$.

Linear classification trains a single linear layer upon extracted image representations for classification. Since the parameter settings of linear classification vary among different baselines, we follow the official parameter settings of each baseline to train its variant under the HIRL framework.

Fine-tuning trains the image encoder along with a linear classifier for classification. We use two sets of parameters for CNN and Vision Transformer based methods, respectively. For CNN based

¹For all tables in this section, we use ‘↑’, ‘→’ and ‘↓’ to denote improvement, equality and degeneration over baseline, respectively. **Bold results** are best within their model type, *i.e.*, CNN or Vision Transformer.

methods, we train with an SGD optimizer (encoder learning rate: 0.1, classifier learning rate: 1.0, weight decay: 0, momentum: 0.9, batch size: 1024) for 20 epochs, and the learning rate is decayed by a factor of 0.2 at the 12th and 16th epoch. For Vision Transformer based methods, we train with an AdamW optimizer (initial learning rate: 4.0×10^{-3} , learning rate layer decay factor [3]: 0.65, weight decay: 0.05, batch size: 1024) and a cosine annealing scheduler [36] for 100 epochs.

Results. In Tab. 2, we report the performance of six baselines and their variants under the HIRL framework. On all three tasks, SwAV and iBOT perform best within CNN and Vision Transformer based approaches, respectively. After adapting into the HIRL framework, performance gain is achieved on all methods and tasks except for HIRL-MoCo v3 on linear classification, and the superiority of SwAV and iBOT still preserves. These results demonstrate that HIRL can indeed boost various image SSL methods by learning extra hierarchical semantic information.

5.2.2 Semi-supervised Learning

Evaluation Setups. *Semi-supervised learning* trains the encoder and a linear classifier on 1% or 10% labeled data of ImageNet. Since MoCo v2 and SimSiam do not evaluate on this task originally, we adopt the official training configurations of SwAV for all three CNN based methods. The training configurations of three Vision Transformer based methods are adapted from their configurations for fine-tuning (Sec. 5.2.1), in which only the initial learning rate is changed for better convergence (semi-1% initial learning rate: 1.0×10^{-3} , semi-10% initial learning rate: 1.0×10^{-4}).

Results. In Tab. 2, we observe that HIRL succeeds in enhancing the performance of all six baselines on both data settings except for HIRL-MoCo v3 on learning with 10% data. In particular, iBOT is improved to achieve a new state-of-the-art performance. Therefore, by acquiring hierarchical image semantics, the pre-trained models show stronger ability of learning from insufficient data.

5.2.3 Transfer Learning

Evaluation Setups. We evaluate on three transfer learning tasks, *i.e.*, classification on Places205 [50], object detection on COCO [34] and instance segmentation on COCO [34]. The configurations of the classification task follow those of fine-tuning (Sec. 5.2.1). For detection and segmentation, the official configurations of MoCo v2 are applied to all CNN based methods, and the official configurations of iBOT are applied to all Vision Transformer based methods. More evaluation details can be found in the Sec. A.3.

Results. According to the comparisons in Tab. 3, all baselines achieve performance gain on all three transfer learning tasks after adapted into HIRL. These improvements verify the strength of HIRL on learning transferable image representations.

5.2.4 Clustering Evaluation

Evaluation Setups. Following iBOT [51], we conduct clustering evaluation on the validation set of ImageNet with 1,000 clusters and measure with three metrics, *i.e.*, accuracy, normalized mutual information (NMI) and adjusted mutual information (AMI). For all CNN based methods, we perform K-means on the average pooled embedding from ResNet. For all Vision Transformer based methods, we perform K-means on the [CLS] token embedding from ViT.

Results. As shown in Tab. 4, HIRL notably boosts the clustering performance of MoCo v2, SimSiam, SwAV, MoCo v3 and iBOT on all three metrics, and it enhances DINO on clustering accuracy. These improvements are mainly attributed to the proposed semantic path discrimination scheme, which can well capture different levels of semantic clusters underlying the raw images.

Table 3: Performance comparison on transfer learning.

Method	Places205 (Top1-Acc)	COCO Det. (AP Box)	COCO Seg. (AP Mask)
CNN based image SSL methods			
MoCo v2	61.4	40.6	35.5
HIRL-MoCo v2	61.9 (↑0.5)	41.1 (↑0.5)	35.7 (↑0.2)
SimSiam	58.4	37.6	33.1
HIRL-SimSiam	61.3 (↑2.9)	40.0 (↑2.4)	35.0 (↑1.9)
SwAV	62.8	39.8	34.6
HIRL-SwAV	63.2 (↑0.4)	40.5 (↑0.7)	35.2 (↑0.6)
Vision Transformer based image SSL methods			
MoCo v3	66.5	48.0	41.7
HIRL-MoCo v3	66.6 (↑0.1)	48.4 (↑0.4)	42.0 (↑0.3)
DINO	66.6	49.7	43.1
HIRL-DINO	67.1 (↑0.5)	50.3 (↑0.6)	43.7 (↑0.6)
iBOT	67.3	50.9	43.9
HIRL-iBOT	67.7 (↑0.4)	51.1 (↑0.2)	44.0 (↑0.1)

Table 4: Performance comparison on clustering evaluation.

Method	Acc	NMI	AMI
CNN based image SSL methods			
MoCo v2	29.3	66.6	41.5
HIRL-MoCo v2	32.9 (↑3.6)	69.4 (↑2.8)	46.5 (↑5.0)
SimSiam	27.9	65.4	39.2
HIRL-SimSiam	30.2 (↑2.3)	66.7 (↑1.3)	41.7 (↑2.5)
SwAV	32.0	67.4	43.0
HIRL-SwAV	33.5 (↑1.5)	68.7 (↑1.3)	45.3 (↑2.3)
Vision Transformer based image SSL methods			
MoCo v3	50.0	78.2	61.9
HIRL-MoCo v3	50.2 (↑0.2)	79.4 (↑1.2)	64.4 (↑2.5)
DINO	50.2	80.8	67.4
HIRL-DINO	52.4 (↑2.2)	80.8 (→)	66.6 (↓0.8)
iBOT	51.1	79.9	64.9
HIRL-iBOT	53.4 (↑2.3)	81.6 (↑1.7)	68.0 (↑3.1)

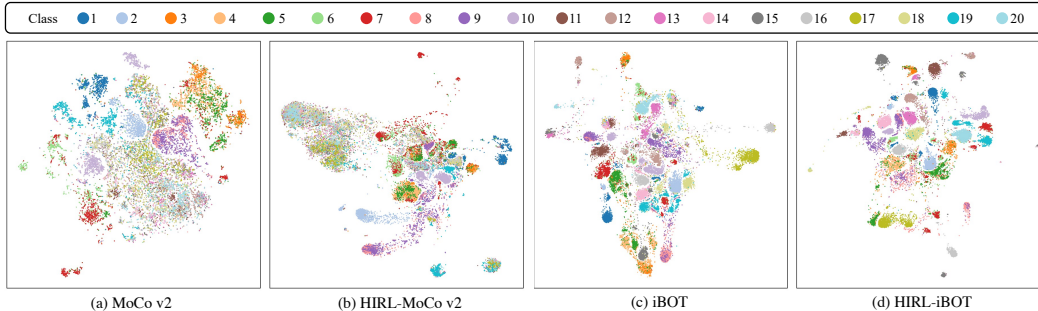


Figure 2: Feature visualization of ImageNet training samples from the first 20 classes.

6 Analysis

6.1 Ablation Study

Effect of prototype structure. In the first block of Tab. 5, we evaluate the HIRL-MoCo v2 trained with different prototype structures. From the 1st, 3rd, 4th and 5th rows, we can observe a monotonic performance increase as the number of prototype layers increases, which demonstrates the effectiveness of learning more levels of semantic information. By comparing the 2nd and 5th rows, it is further shown that learning with multiple layers of prototypes is more effective than learning with a single layer of more prototypes (*i.e.*, $50000 > 30000 + 10000 + 1000 + 200$).

Effect of negative path sampling. The second block of Tab. 5 studies the effect of negative path sampling on HIRL-MoCo v2. The results illustrate that the objective function of semantic path discrimination (Eq. (3)) is comparably effective under a wide range of negative path sampling sizes.

6.2 Time Complexity Analysis

Compared to a baseline, its variant under HIRL requires an additional hierarchical K-means step per epoch, whose time complexity is $\mathcal{O}(NM_1d + \sum_{l=1}^{L-1} M_l M_{l+1} d) = \mathcal{O}(NM_1d)$ (N : dataset size, M_l : prototype number at the l -th semantic level, d : representation dimension). This step makes up of the majority of HIRL’s extra computation. Since N and M_1 are identical among different methods, a larger d will lead to higher extra cost, which is verified by the results in Tab. 6.

6.3 Visualization

In Fig. 2, we use t-SNE [28] to visualize image representations. We randomly sample 2,000 images from each of the first 20 classes of ImageNet training set for visualization. Compared to the original MoCo v2 and iBOT, the image representations of different classes are better separated after trained under the HIRL framework. For example, the original iBOT confuses the representations of class 18 and 20, while these two classes are well divided by HIRL-iBOT in the latent space.

7 Conclusions and Future Work

This work proposes a general framework for Hierarchical Image Representation Learning (HIRL). It acquires the most fine-grained semantics by an arbitrary off-the-shelf image SSL method, and it learns more coarse-grained semantic information by semantic path discrimination. HIRL succeeds in enhancing six representative image SSL approaches on a broad range of downstream tasks.

The main limitation of the current HIRL framework is that it can only learn the semantics of individual visual objects, while the interactions between different objects are not well captured. Therefore, our future work will mainly focus on designing an SSL method that can jointly capture the semantics of visual objects and their interactions.

Table 5: Ablation study for prototype structure and negative path sampling. (All results are reported on HIRL-MoCo v2.)

# Prototypes	# Negative paths	KNN (Top1-Acc)
(30000)	1000	56.22
(50000)	1000	56.71
(30000, 10000)	1000	56.75
(30000, 10000, 1000)	1000	57.56
(30000, 10000, 1000, 200)	1000	57.72
(30000, 10000, 1000)	100	57.28
(30000, 10000, 1000)	1000	57.56
(30000, 10000, 1000)	5000	57.37
(30000, 10000, 1000)	10000	57.32

Table 6: Running time comparison.

Method	Dimension	Per-epoch runtime
MoCo v2	128	13min 39s
HIRL-MoCo v2	128	17min 30s
SimSiam	2048	12min 9s
HIRL-SimSiam	2048	21min 10s
SwAV	128	6min 3s
HIRL-SwAV	128	8min 15s
MoCo v3	256	3min 58s
HIRL-MoCo v3	256	6min 30s
DINO	256	13min 0s
HIRL-DINO	256	16min 9s
iBOT	256	13min 6s
HIRL-iBOT	256	16min 10s

References

- [1] Yuki Markus Asano, Christian Rupprecht, and Andrea Vedaldi. Self-labelling via simultaneous clustering and representation learning. *arXiv preprint arXiv:1911.05371*, 2019.
- [2] Alexei Baevski, Wei-Ning Hsu, Qiantong Xu, Arun Babu, Jiatao Gu, and Michael Auli. data2vec: A general framework for self-supervised learning in speech, vision and language. *arXiv preprint arXiv:2202.03555*, 2022.
- [3] Hangbo Bao, Li Dong, and Furu Wei. Beit: Bert pre-training of image transformers. *arXiv preprint arXiv:2106.08254*, 2021.
- [4] Zhaowei Cai and Nuno Vasconcelos. Cascade r-cnn: High quality object detection and instance segmentation. *IEEE Transactions on Pattern Analysis and Machine Intelligence*, 43(5):1483–1498, 2019.
- [5] Mathilde Caron, Piotr Bojanowski, Armand Joulin, and Matthijs Douze. Deep clustering for unsupervised learning of visual features. In *European Conference on Computer Vision*, 2018.
- [6] Mathilde Caron, Piotr Bojanowski, Julien Mairal, and Armand Joulin. Unsupervised pre-training of image features on non-curated data. In *International Conference on Computer Vision*, 2019.
- [7] Mathilde Caron, Ishan Misra, Julien Mairal, Priya Goyal, Piotr Bojanowski, and Armand Joulin. Unsupervised learning of visual features by contrasting cluster assignments. In *Advances in Neural Information Processing Systems*, 2020.
- [8] Mathilde Caron, Hugo Touvron, Ishan Misra, Hervé Jégou, Julien Mairal, Piotr Bojanowski, and Armand Joulin. Emerging properties in self-supervised vision transformers. In *International Conference on Computer Vision*, 2021.
- [9] Kai Chen, Jiaqi Wang, Jiangmiao Pang, Yuhang Cao, Yu Xiong, Xiaoxiao Li, Shuyang Sun, Wansen Feng, Ziwei Liu, Jiarui Xu, et al. Mmdetection: Open mmlab detection toolbox and benchmark. *arXiv preprint arXiv:1906.07155*, 2019.
- [10] Mark Chen, Alec Radford, Rewon Child, Jeffrey Wu, Heewoo Jun, David Luan, and Ilya Sutskever. Generative pretraining from pixels. In *International Conference on Machine Learning*, 2020.
- [11] Ting Chen, Simon Kornblith, Mohammad Norouzi, and Geoffrey E. Hinton. A simple framework for contrastive learning of visual representations. In *International Conference on Machine Learning*, 2020.
- [12] Tsai-Shien Chen, Wei-Chih Hung, Hung-Yu Tseng, Shao-Yi Chien, and Ming-Hsuan Yang. Incremental false negative detection for contrastive learning. *arXiv preprint arXiv:2106.03719*, 2021.
- [13] Xiaokang Chen, Mingyu Ding, Xiaodi Wang, Ying Xin, Shentong Mo, Yunhao Wang, Shumin Han, Ping Luo, Gang Zeng, and Jingdong Wang. Context autoencoder for self-supervised representation learning. *arXiv preprint arXiv:2202.03026*, 2022.
- [14] Xinlei Chen, Haoqi Fan, Ross Girshick, and Kaiming He. Improved baselines with momentum contrastive learning. *arXiv preprint arXiv:2003.04297*, 2020.
- [15] Xinlei Chen and Kaiming He. Exploring simple siamese representation learning. In *International Conference on Computer Vision*, 2021.
- [16] Xinlei Chen, Saining Xie, and Kaiming He. An empirical study of training self-supervised vision transformers. In *International Conference on Computer Vision*, 2021.
- [17] Ching-Yao Chuang, Joshua Robinson, Yen-Chen Lin, Antonio Torralba, and Stefanie Jegelka. Debaised contrastive learning. In *Advances in Neural Information Processing Systems*, 2020.
- [18] Jia Deng, Wei Dong, Richard Socher, Li-Jia Li, Kai Li, and Li Fei-Fei. Imagenet: A large-scale hierarchical image database. In *IEEE Conference on Computer Vision and Pattern Recognition*, 2009.
- [19] Jacob Devlin, Ming-Wei Chang, Kenton Lee, and Kristina Toutanova. Bert: Pre-training of deep bidirectional transformers for language understanding. *arXiv preprint arXiv:1810.04805*, 2018.

- [20] Alexey Dosovitskiy, Lucas Beyer, Alexander Kolesnikov, Dirk Weissenborn, Xiaohua Zhai, Thomas Unterthiner, Mostafa Dehghani, Matthias Minderer, Georg Heigold, Sylvain Gelly, et al. An image is worth 16x16 words: Transformers for image recognition at scale. *arXiv preprint arXiv:2010.11929*, 2020.
- [21] Spyros Gidaris, Praveer Singh, and Nikos Komodakis. Unsupervised representation learning by predicting image rotations. In *International Conference on Learning Representations*, 2018.
- [22] Jean-Bastien Grill, Florian Strub, Florent Alché, Corentin Tallec, Pierre H Richemond, Elena Buchatskaya, Carl Doersch, Bernardo Avila Pires, Zhaohan Daniel Guo, Mohammad Gheshlaghi Azar, et al. Bootstrap your own latent: A new approach to self-supervised learning. *arXiv preprint arXiv:2006.07733*, 2020.
- [23] Yuanfan Guo, Minghao Xu, Jiawen Li, Bingbing Ni, Xuanyu Zhu, Zhenbang Sun, and Yi Xu. Hcsc: Hierarchical contrastive selective coding. *arXiv preprint arXiv:2202.00455*, 2022.
- [24] Kaiming He, Xinlei Chen, Saining Xie, Yanghao Li, Piotr Dollár, and Ross Girshick. Masked autoencoders are scalable vision learners. *arXiv preprint arXiv:2111.06377*, 2021.
- [25] Kaiming He, Haoqi Fan, Yuxin Wu, Saining Xie, and Ross B. Girshick. Momentum contrast for unsupervised visual representation learning. In *IEEE Conference on Computer Vision and Pattern Recognition*, 2020.
- [26] Kaiming He, Georgia Gkioxari, Piotr Dollár, and Ross Girshick. Mask r-cnn. In *International Conference on Computer Vision*, 2017.
- [27] Kaiming He, Xiangyu Zhang, Shaoqing Ren, and Jian Sun. Deep residual learning for image recognition. In *International Conference on Computer Vision*, 2016.
- [28] Geoffrey Hinton and Sam T Roweis. Stochastic neighbor embedding. In *Advances in Neural Information Processing Systems*, 2002.
- [29] R Devon Hjelm, Alex Fedorov, Samuel Lavoie-Marchildon, Karan Grewal, Phil Bachman, Adam Trischler, and Yoshua Bengio. Learning deep representations by mutual information estimation and maximization. *arXiv preprint arXiv:1808.06670*, 2018.
- [30] Qianjiang Hu, Xiao Wang, Wei Hu, and Guo-Jun Qi. Adco: Adversarial contrast for efficient learning of unsupervised representations from self-trained negative adversaries. In *International Conference on Computer Vision*, 2021.
- [31] Gustav Larsson, Michael Maire, and Gregory Shakhnarovich. Learning representations for automatic colorization. In *European Conference on Computer Vision*, 2016.
- [32] Junnan Li, Pan Zhou, Caiming Xiong, Richard Socher, and Steven C. H. Hoi. Prototypical contrastive learning of unsupervised representations. In *International Conference on Learning Representations*, 2021.
- [33] Tsung-Yi Lin, Piotr Dollár, Ross Girshick, Kaiming He, Bharath Hariharan, and Serge Belongie. Feature pyramid networks for object detection. In *IEEE Conference on Computer Vision and Pattern Recognition*, 2017.
- [34] Tsung-Yi Lin, Michael Maire, Serge Belongie, James Hays, Pietro Perona, Deva Ramanan, Piotr Dollár, and C Lawrence Zitnick. Microsoft coco: Common objects in context. In *European Conference on Computer Vision*, 2014.
- [35] Ze Liu, Yutong Lin, Yue Cao, Han Hu, Yixuan Wei, Zheng Zhang, Stephen Lin, and Baining Guo. Swin transformer: Hierarchical vision transformer using shifted windows. In *International Conference on Computer Vision*, 2021.
- [36] Ilya Loshchilov and Frank Hutter. Sgdr: Stochastic gradient descent with warm restarts. *arXiv preprint arXiv:1608.03983*, 2016.
- [37] Mehdi Noroozi and Paolo Favaro. Unsupervised learning of visual representations by solving jigsaw puzzles. In *European Conference on Computer Vision*, 2016.
- [38] Adam Paszke, Sam Gross, Soumith Chintala, Gregory Chanan, Edward Yang, Zachary DeVito, Zeming Lin, Alban Desmaison, Luca Antiga, and Adam Lerer. Automatic differentiation in pytorch. In *NeurIPS Workshop*, 2017.
- [39] Shaoqing Ren, Kaiming He, Ross Girshick, and Jian Sun. Faster r-cnn: Towards real-time object detection with region proposal networks. In *Advances in Neural Information Processing Systems*, 2015.

- [40] Hugo Touvron, Matthieu Cord, Matthijs Douze, Francisco Massa, Alexandre Sablayrolles, and Hervé Jégou. Training data-efficient image transformers & distillation through attention. In *International Conference on Machine Learning*, 2021.
- [41] Aäron van den Oord, Yazhe Li, and Oriol Vinyals. Representation learning with contrastive predictive coding. *arXiv preprint arXiv:1807.03748*, 2018.
- [42] Xiao Wang and Guo-Jun Qi. Contrastive learning with stronger augmentations. *arXiv preprint arXiv:2104.07713*, 2021.
- [43] Zhirong Wu, Yuanjun Xiong, Stella X Yu, and Dahua Lin. Unsupervised feature learning via non-parametric instance discrimination. In *IEEE Conference on Computer Vision and Pattern Recognition*, 2018.
- [44] Junyuan Xie, Ross Girshick, and Ali Farhadi. Unsupervised deep embedding for clustering analysis. In *International Conference on Machine Learning*, 2016.
- [45] Zhenda Xie, Zheng Zhang, Yue Cao, Yutong Lin, Jianmin Bao, Zhuliang Yao, Qi Dai, and Han Hu. Simmim: A simple framework for masked image modeling. *arXiv preprint arXiv:2111.09886*, 2021.
- [46] Jianwei Yang, Devi Parikh, and Dhruv Batra. Joint unsupervised learning of deep representations and image clusters. In *IEEE Conference on Computer Vision and Pattern Recognition*, 2016.
- [47] Yang You, Igor Gitman, and Boris Ginsburg. Large batch training of convolutional networks. *arXiv preprint arXiv:1708.03888*, 2017.
- [48] Jure Zbontar, Li Jing, Ishan Misra, Yann LeCun, and Stéphane Deny. Barlow twins: Self-supervised learning via redundancy reduction. *arXiv preprint arXiv:2103.03230*, 2021.
- [49] Richard Zhang, Phillip Isola, and Alexei A Efros. Colorful image colorization. In *European Conference on Computer Vision*, 2016.
- [50] Bolei Zhou, Agata Lapedriza, Jianxiong Xiao, Antonio Torralba, and Aude Oliva. Learning deep features for scene recognition using places database. In *Advances in Neural Information Processing Systems*, 2014.
- [51] Jinghao Zhou, Chen Wei, Huiyu Wang, Wei Shen, Cihang Xie, Alan Yuille, and Tao Kong. ibot: Image bert pre-training with online tokenizer. *arXiv preprint arXiv:2111.07832*, 2021.

A More Implementation Details

A.1 Adaptation of Baselines to the HIRL Framework

In the main paper, we introduce how each baseline method is adapted into the HIRL framework from two aspects, feature extraction and loss computation. For feature extraction, HIRL deems the image representation extracted by the baseline model as the representation z^0 for most fine-grained semantics. Based on this representation, HIRL discovers hierarchical prototypes and derives the representations $\{z^l\}_{l=1}^L$ for more coarse-grained semantics. Here, we specifically state which layer’s output of each baseline method serves as the representation z^0 .

- **MoCo v2 [14]** uses a 2-layer MLP to project the average pooled embedding of ResNet to the semantic space for contrastive learning. Under the HIRL framework, we regard the output of this projection head as z^0 .
- **SimSiam [15]** employs a 3-layer MLP to project the average pooled embedding of ResNet to the semantic space for cross-view prediction. We adopt this projection head’s output as z^0 . Upon the projection head, SimSiam involves another MLP as the predictor, while it is not used to derive hierarchical semantic representations.
- **SwAV [7]** uses a 2-layer MLP to project the average pooled embedding of ResNet to the semantic space for cluster assignment prediction. The projected embedding serves as z^0 under HIRL.
- **MoCo v3 [16]** utilizes a 3-layer MLP to project the [CLS] token embedding of ViT to the semantic space for contrastive learning. We deem the output of this projection head as z^0 . Similar as SimSiam, MoCo v3 defines an MLP predictor upon the projection head for cross-view prediction. This predictor is not used to derive hierarchical semantic representations.
- **DINO [8]** employs a 3-layer MLP to project the [CLS] token embedding of ViT to the semantic space for self-distillation. The output of this projection head is deemed as z^0 under HIRL.
- **iBOT [51]** uses a 3-layer MLP to project the [CLS] token embedding of ViT to the semantic space for self-distillation and masked image modeling. We adopt the projected embedding as z^0 .

A.2 More Training Details

Table 7: More training configurations of baselines and their variants under HIRL.

Method	Optimizer	Init. learning rate	Learning rate scheduler
MoCo v2	SGD (momentum: 0.9, weight decay: 1.0×10^{-4})	0.03	cosine anneal (min. lr: 0)
HIRL-MoCo v2	SGD (momentum: 0.9, weight decay: 1.0×10^{-4})	0.03	cosine anneal (min. lr: 0)
SimSiam	SGD (momentum: 0.9, weight decay: 1.0×10^{-4})	0.1	cosine anneal (min. lr: 0)
HIRL-SimSiam	SGD (momentum: 0.9, weight decay: 1.0×10^{-4})	0.1	cosine anneal (min. lr: 0)
SwAV	SGD (momentum: 0.9, weight decay: 1.0×10^{-6}) + LARS [47]	4.8	10 epochs warmup (lr: $0.3 \rightarrow 4.8$) + cosine anneal (min. lr: 4.8×10^{-3})
HIRL-SwAV	SGD (momentum: 0.9, weight decay: 1.0×10^{-6}) + LARS [47]	4.8	10 epochs warmup (lr: $0.3 \rightarrow 4.8$) + cosine anneal (min. lr: 4.8×10^{-3})
MoCo v3	AdamW (betas: [0.9, 0.999], weight decay: 0.1)	1.6×10^{-3}	40 epochs warmup (lr: $0 \rightarrow 1.6 \times 10^{-3}$) + cosine anneal (min. lr: 0)
HIRL-MoCo v3	AdamW (betas: [0.9, 0.999], weight decay: 0.1)	1.6×10^{-3}	40 epochs warmup (lr: $0 \rightarrow 1.6 \times 10^{-3}$) + cosine anneal (min. lr: 0)
DINO	AdamW (betas: [0.9, 0.999], weight decay: $0.04 \rightarrow 0.4$ †)	3.0×10^{-3}	10 epochs warmup (lr: $0 \rightarrow 3.0 \times 10^{-3}$) + cosine anneal (min. lr: 2.0×10^{-6})
HIRL-DINO	AdamW (betas: [0.9, 0.999], weight decay: $0.04 \rightarrow 0.4$ †)	3.0×10^{-3}	10 epochs warmup (lr: $0 \rightarrow 3.0 \times 10^{-3}$) + cosine anneal (min. lr: 2.0×10^{-6})
iBOT	AdamW (betas: [0.9, 0.999], weight decay: $0.04 \rightarrow 0.4$ †)	3.0×10^{-3}	10 epochs warmup (lr: $0 \rightarrow 3.0 \times 10^{-3}$) + cosine anneal (min. lr: 2.0×10^{-6})
HIRL-iBOT	AdamW (betas: [0.9, 0.999], weight decay: $0.04 \rightarrow 0.4$ †)	3.0×10^{-3}	10 epochs warmup (lr: $0 \rightarrow 3.0 \times 10^{-3}$) + cosine anneal (min. lr: 2.0×10^{-6})

† Weight decay is not applied on bias and normalization parameters; the weight decay rate increases from 0.04 to 0.4 along training.

In Tab. 7, we list the optimizer, initial learning rate and learning rate scheduler for each baseline and its variant under HIRL. In general, we follow the official implementation to set the configurations of each baseline, and the adaptation to the HIRL framework does not change any training configuration, which ensures fair comparison. We state the extra configurations specific to each method as below.

- **MoCo v2** constructs a single positive pair per sample for contrastive learning. Each view of a pair is transformed from the raw image by a sequential of random crop, resize to 224×224 , color transformation and random horizontal flip. We refer readers to the original paper [14] for detailed parameters of each transformation function. MoCo v2 maintains a queue of 65,536 image embeddings as negative samples. For a positive pair, the embedding of one of its view is extracted by a vanilla encoder updated by gradients per training step, and the embedding of another view is extracted by a momentum encoder whose parameters are the moving average of the vanilla encoder’s parameters, where the momentum is set as 0.999.
- **SimSiam** also uses a single positive pair per sample for cross-view prediction. Its transformation scheme for each view of a pair follows that of MoCo v2. The learning of SimSiam does not rely on negative pairs.

- **SwAV** constructs 2 global views and 6 local views per sample to perform cross-view cluster assignment prediction. Both the global and local views of an image are derived by sequentially applying random crop, resize, color transformation and random horizontal flip. The global view is resized to 224×224 , and the local view is resized to 96×96 . We refer readers to the original paper [7] for other transformation parameters.
- **MoCo v3** follows MoCo v2 to derive positive pairs. However, instead of maintaining a queue of negative samples as in MoCo v2, it utilizes other samples in a mini-batch to construct negative pairs, which is demonstrated to be better when training with large batch size. MoCo v3 also maintains a momentum encoder along training, where the value of momentum increases from 0.99 to 1 with a cosine rate.
- **DINO** constructs 2 global views and 10 local views per sample for self-distillation across different views. Both the global and local views are derived by a sequential of random crop, resize, random horizontal flip and color transformation. The global view is resized to 224×224 , and the local view is resized to 96×96 . Readers are referred to the original paper [8] for other transformation parameters. DINO maintains a teacher network as the moving average of the student network, where the momentum for updating the teacher network increases from 0.996 to 1 along the training process with a cosine rate. Also, DINO uses the momentum update scheme to maintain the center value of each representation dimension, in which the momentum is set as 0.9.
- **iBOT** follows DINO to derive local and global views for self-distillation and masked image modeling. iBOT also maintains a teacher network and center values of image representations following the schemes in DINO. iBOT additionally maintains a center value for each dimension of patch representation by momentum update, where the momentum is set as 0.9.

A.3 More Evaluation Details of Transfer Learning

We apply the detection and segmentation configurations of MoCo v2 [14] to all CNN based methods, and the configurations of iBOT [51] are applied to all Vision Transformer based methods.

Object detection for CNN based methods. For object detection on COCO [34], we employ the Faster-RCNN-C4 [39] as the object detector and initialize it with the model weights pre-trained by different methods. We train the model on the train2017 split of COCO and evaluate on the val2017 split. An SGD optimizer (initial learning rate: 0.02, weight decay: 1.0×10^{-4} , momentum: 0.9, batch size: 16) is used to train the model for 180,000 iterations, and the learning rate is warmed up for 100 iterations and decayed by a factor of 0.1 at the 120,000th and 160,000th iteration.

Instance segmentation for CNN based methods. For instance segmentation on COCO, as in Mask R-CNN [26], we basically follow the model architecture for object detection and additionally append a mask prediction head for segmentation. All training configurations are identical between the detection task and the segmentation task.

Object detection for Vision Transformer based methods. We utilize the MMDetection toolbox [9] to evaluate various pre-trained Vision Transformers on COCO object detection. The object detector is built under the Cascade Mask R-CNN architecture [4], where the outputs of ViT-B/16 [20] at the 4th, 6th, 8th and 12th Transformer block serve as the inputs of the Feature Pyramid Network (FPN) [33]. We employ an AdamW optimizer (betas: [0.9, 0.999], weight decay: 0.05, learning rate layer decay factor [3]: 0.65, batch size: 16) to train the model for 12 epochs. The initial learning rate is set as 1.6×10^{-4} for MoCo v3 and is set as 1.0×10^{-4} for DINO and iBOT, and the learning rate is decayed by a factor of 0.1 at the 9th and 11th epoch. We follow the multi-scale training scheme used in iBOT, and the multi-scale test is not applied.

Instance segmentation for Vision Transformer based methods. Also, for COCO instance segmentation with Vision Transformer, we append a mask prediction head to the Vision Transformer based detection model for segmentation, which follows the design of Mask R-CNN. All training configurations are aligned between detection and segmentation.

B Results of Longer Training on SwAV

In the original paper of SwAV [7], researchers achieve performance gain by increasing pre-training epochs. Here, we want to (1) reproduce this phenomenon under our codebase and (2) verify that the superiority of HIRL-SwAV over the original SwAV preserves as the increase of pre-training epochs.

Table 8: Results of SwAV and HIRL-SwAV under 200/800 epochs training. Downstream tasks: KNN evaluation (Top1-Acc), linear classification (Top1-Acc), fine-tuning (Top1-Acc) and semi-supervised learning with 1% or 10% data (Top1-Acc). We use Tesla-V100-32GB GPUs for all experiments.

Method	Arch.	# Epochs	Batch size	# GPUs	Train time	KNN	Linear	Fine-tune	Semi-1%	Semi-10%
SwAV	ResNet-50	200	4096	32	20h 15min	63.45	72.68	76.82	51.23	68.72
HIRL-SwAV	ResNet-50	200	4096	32	27h 45min	63.99 (\uparrow 0.54)	73.43 (\uparrow 0.75)	77.18 (\uparrow 0.36)	52.12 (\uparrow 0.89)	69.32 (\uparrow 0.60)
SwAV	ResNet-50	800	4096	32	81h 2min	64.84	73.36	77.77	52.72	70.15
HIRL-SwAV	ResNet-50	800	4096	32	107h 30min	65.43 (\uparrow 0.59)	74.80 (\uparrow 1.44)	78.05 (\uparrow 0.28)	53.92 (\uparrow 1.20)	70.62 (\uparrow 0.47)

Training Setups. We investigate SwAV and HIRL-SwAV under 200 and 800 pre-training epochs, respectively. Except for the pre-training epochs, we keep all other training configurations invariant (see Sec. A.2 for detailed configurations of SwAV). Under 200 epochs pre-training, HIRL-SwAV takes the first 20 epochs as the first-stage training (*i.e.*, training with only SwAV’s objective) and takes the rest epochs as the second-stage training (*i.e.*, training with both SwAV’s objective and the objective for semantic path discrimination). Under 800 epochs pre-training, the first 80 epochs serve as the first stage, and the rest epochs serve as the second stage.

When pre-trained for 200 epochs, HIRL-SwAV adopts 3-layer hierarchical prototypes with prototype numbers $(M_1, M_2, M_3) = (30000, 10000, 1000)$, and 1000 negative paths are sampled for semantic path discrimination. When pre-trained for 800 epochs, HIRL-SwAV uses the hierarchical prototype structure $(M_1, M_2, M_3) = (30000, 10000, 1000)$ and the negative path sampling size 1000. These hyperparameters are determined by the search scheme described in Sec. 5.1.3. Under both 200 and 800 epochs pre-training, we implement the projection heads h_l ($1 \leq l \leq L$) as 2-layer MLPs with batch normalization and ReLU activation in between.

Evaluation Setups. We evaluate pre-trained models with five standard downstream tasks, *i.e.*, KNN evaluation, linear classification, fine-tuning and semi-supervised learning with 1% or 10% data. All these tasks are evaluated on the ImageNet [18] dataset following respective evaluation protocols.

Results. In Tab. 8, we report the performance of SwAV and HIRL-SwAV under 200 and 800 epochs pre-training, respectively. The SwAV model trained for 800 epochs clearly outperforms its 200 epochs counterpart on all five tasks, which aligns with the original paper’s finding that longer training benefits the performance of SwAV [7]. Under both 200 and 800 epochs pre-training, HIRL-SwAV surpasses the SwAV baseline with a clear margin on all five tasks. These improvements demonstrate that HIRL can boost off-the-shelf image SSL methods under different training length.

C More Visualization Results

In Figs. 3 and 4, we visualize two typical semantic subtrees within the whole hierarchical prototypes constructed by HIRL-DINO. Each node of a subtree denotes a semantic prototype which is represented by some images assigned to it. The tree in Fig. 3 discovers the semantic hierarchy of vehicles, *i.e.*, “vehicle \rightarrow car \rightarrow sport car”, “vehicle \rightarrow car \rightarrow taxi”, “vehicle \rightarrow ship \rightarrow sailboat” and “vehicle \rightarrow ship \rightarrow steamship”. The tree in Fig. 4 discovers the semantic hierarchy of containers, *i.e.*, “container \rightarrow tea set \rightarrow cup”, “container \rightarrow tea set \rightarrow pot”, “container \rightarrow art craft \rightarrow vase” and “container \rightarrow art craft \rightarrow ceramics”. These results illustrate that, under the proposed HIRL framework, image SSL methods can indeed capture hierarchical semantic information.

D Broader Societal Impacts

This work focuses on designing a general framework to acquire the hierarchical semantic information underlying raw images. This framework learns the model in a totally self-supervised way, which relieves the heavy labor of annotating training samples. Compared to existing self-supervised methods, our approach can acquire more levels of image semantics, which can potentially benefit a broader range of industry applications, like intelligent surveillance under different safety levels.

However, it cannot be denied that the training process under our framework is time- and resource-intensive. For example, the training of MoCo v2 [14] takes 19.6 GPU days under our framework, which is more expensive than the 15.1 GPU days training of the original MoCo v2. Therefore, how to train an effective self-supervised image representation model in a more computationally efficient way remains to be further explored. Our future work will seek to address this problem by designing more data-efficient models and training with less data.

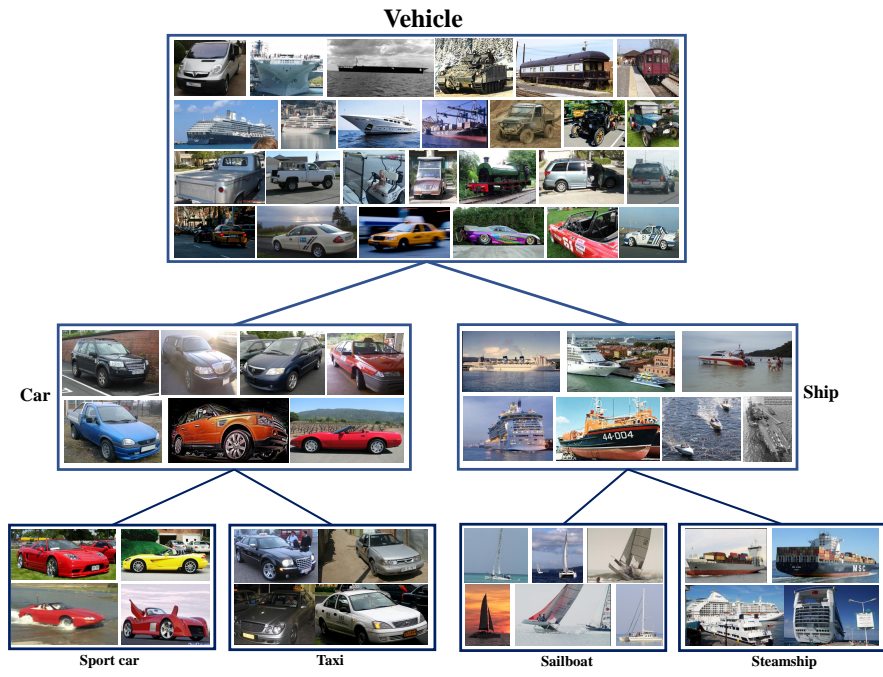


Figure 3: A semantic subtree discovered by HIRL-DINO.

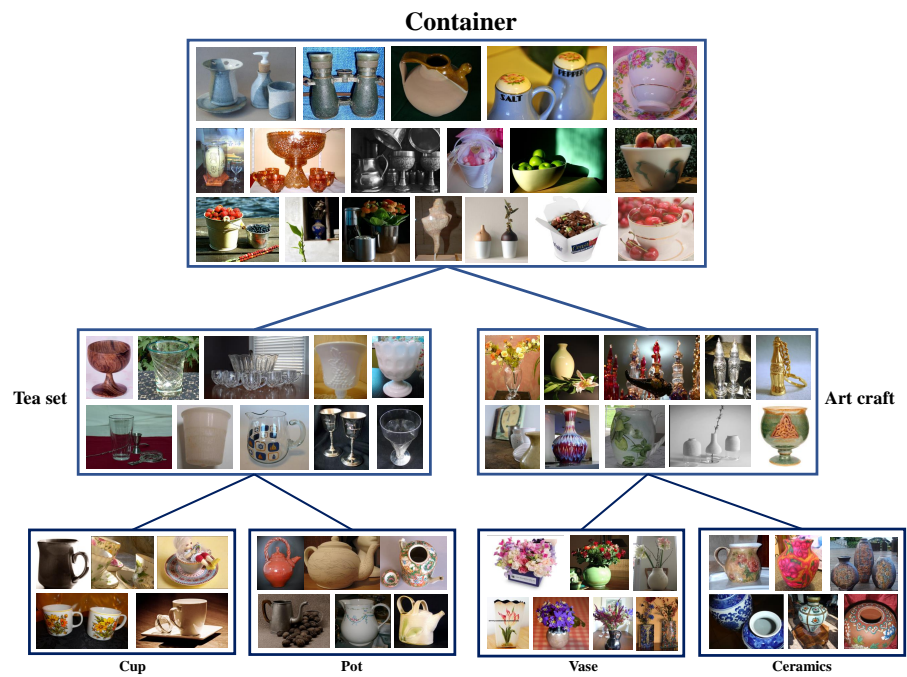


Figure 4: Another semantic subtree discovered by HIRL-DINO.